

SDG2-Mediated H3K4me3 Is Crucial for Chromatin Condensation and Mitotic Division during Male Gametogenesis in Arabidopsis^{1[OPEN]}

Violaine Pinon², Xiaozhen Yao², Aiwu Dong, and Wen-Hui Shen*

Université de Strasbourg, Centre National de la Recherche Scientifique UPR2357, F-67000 Strasbourg, France (V.P., W.-H.S.); State Key Laboratory of Genetic Engineering, Collaborative Innovation Center of Genetics and Development, International Associated Laboratory of Centre National de la Recherche Scientifique-Fudan-HUNAU on Plant Epigenome Research, Department of Biochemistry, Institute of Plant Biology, School of Life Sciences, Fudan University, Shanghai 200433, China (X.Y., A.D., W.-H.S.); and College of Life and Environment Sciences, Shanghai Normal University, Shanghai 200234, China (X.Y.)

ORCID IDs: 0000-0002-2075-4235 (A.D.); 0000-0001-7988-6382 (W.-H.S.).

Epigenetic reprogramming occurring during reproduction is crucial for both animal and plant development. Histone H3 Lys 4 trimethylation (H3K4me3) is an evolutionarily conserved epigenetic mark of transcriptional active euchromatin. While much has been learned in somatic cells, H3K4me3 deposition and function in gametophyte is poorly studied. Here, we demonstrate that SET DOMAIN GROUP2 (SDG2)-mediated H3K4me3 deposition participates in epigenetic reprogramming during Arabidopsis male gametogenesis. We show that loss of SDG2 barely affects meiosis and cell fate establishment of haploid cells. However, we found that SDG2 is critical for postmeiotic microspore development. Mitotic cell division progression is partly impaired in the loss-of-function *sdg2-1* mutant, particularly at the second mitosis setting up the two sperm cells. We demonstrate that SDG2 is involved in promoting chromatin decondensation in the pollen vegetative nucleus, likely through its role in H3K4me3 deposition, which prevents ectopic heterochromatic H3K9me2 speckle formation. Moreover, we found that derepression of the LTR retrotransposon *ATLANTYS1* is compromised in the vegetative cell of the *sdg2-1* mutant pollen. Consistent with chromatin condensation and compromised transcription activity, pollen germination and pollen tube elongation, representing the key function of the vegetative cell in transporting sperm cells during fertilization, are inhibited in the *sdg2-1* mutant. Taken together, we conclude that SDG2-mediated H3K4me3 is an essential epigenetic mark of the gametophyte chromatin landscape, playing critical roles in gamete mitotic cell cycle progression and pollen vegetative cell function during male gametogenesis and beyond.

In animals and plants, epigenetic reprogramming during reproduction is believed to play crucial roles in maintaining genome integrity, in potentiating genetic

and epigenetic variation, in resetting gene-expression program, and in contributing to the embryo totipotency at fertilization (Sasaki and Matsui, 2008; Feng et al., 2010; Kawashima and Berger, 2014; Lesch and Page, 2014). In animals, a diploid germline arises early during embryogenesis and remains as a distinct niche of stem cells (primordial germ cells) throughout life (Sasaki and Matsui, 2008). In flowering plants, however, the germline is differentiated from somatic cells within specialized organs of the flower, which is formed late in development, after a long postembryonic phase of plant growth (Ma, 2005). Furthermore, while in animals gametes are direct products of meiosis, in plants multicellular haploid gametophytes are formed through rounds of postmeiotic cell divisions. Thus, in many flowering plants including the model plant Arabidopsis (*Arabidopsis thaliana*), the male gametophyte is characterized by a three-celled pollen and the female gametophyte by a seven-celled embryo sac (Berger and Twell, 2011; Schmid et al., 2015). Upon double fertilization, one of the two haploid sperm cells from the pollen fuses with the egg cell of the embryo sac to form the diploid zygote, which develops into embryo. The

¹ This work was supported by the French Agence Nationale de la Recherche (ANR-12-BSV2-0013-02), the National Basic Research Program of China (973 Program, 2012CB910500 and 2011CB944600), the National Natural Science Foundation of China (grants 31571319, 31371304, and 31300263), the Science and Technology Commission of Shanghai Municipality (grant 13JC1401000), and the French Centre National de la Recherche Scientifique (CNRS, LIA PER).

² These authors contributed equally to the article.

* Address correspondence to wen-hui.shen@ibmp-cnrs.unistra.fr.

The author responsible for distribution of materials integral to the findings presented in this article in accordance with the policy described in the Instructions for Authors (www.plantphysiol.org) is: Wen-Hui Shen (wen-hui.shen@ibmp-cnrs.unistra.fr).

W.-H.S. conceived the original research plans and supervised the experiments; V.P. and X.Y. performed the experiments and analyzed the data with equal contribution; A.D. provided assistance to X.Y. and supervised some of the experiments; V.P., X.Y., and W.-H.S. wrote the article with contributions from all the authors.

^[OPEN] Articles can be viewed without a subscription.

www.plantphysiol.org/cgi/doi/10.1104/pp.17.00306

other sperm cell fuses with the central cell of the embryo sac to produce the triploid endosperm, a tissue providing nourishment to the developing embryo (Hamamura et al., 2012). These differences of reproductive strategies used by plants as compared to animals are driving intense interest on epigenetic reprogramming mechanisms associated with complex cell fate establishment and maintenance during plant reproduction.

Cell-type specificities lay in distinctive transcriptomes that are controlled by the activity of transcription factors and by the chromatin structure, which can impede the accessibility and activity of the transcriptional machinery. In mammals, an erasure of almost all DNA methylation states is observed before fertilization (Feng et al., 2010). In plants, however, such an extreme reprogramming event does not seem to occur at fertilization (Ingouff et al., 2017; Saze et al., 2003; Jullien et al., 2012; Calarco et al., 2012). Moreover, over 85% of mammalian histones are replaced by sperm-specific protamine proteins, enabling extensive compaction of DNA in male gametes, and upon fertilization the paternal chromatin is deprived of the protamines and loaded with variant histone H3.3 provided by the female gametes (Ooi and Henikoff, 2007; Saitou and Kurimoto, 2014). However, plants do not contain protamines, and in Arabidopsis germ cells, the canonical histone H3.1 is replaced by the H3.3 variant, HISTONE THREE RELATED10 (HTR10), which is subsequently removed from the zygote nucleus upon fertilization (Ingouff et al., 2007, 2010). Within pollen, chromatin is less condensed in the vegetative cell nucleus than in the two sperm cell nuclei. Interestingly, during microsporogenesis, DNA demethylation occurs in the pollen vegetative cell nucleus and activation of transposable elements (TEs) in the vegetative cell has been proposed to generate small RNAs to reinforce silencing of complementary TEs in sperm cells (Ibarra et al., 2012; Slotkin et al., 2009; Calarco et al., 2012). Moreover, the heterochromatin mark H3K9me2 specifically accumulates in the two sperm cell nuclei, while it is greatly absent from the vegetative cell nucleus (Schoft et al., 2009), and the other histone methylations including H3K4me2/me3, H3K36me2/me3, and H3K27me3 are detected abundantly in the vegetative cell nucleus (Cartagena et al., 2008; Sano and Tanaka, 2010; Houben et al., 2011; Pandey et al., 2013).

Methylation of histone Lys residues depends on the activity of histone methyltransferases (HMTases): Most of them contain an evolutionarily conserved catalytic SET domain (Huang et al., 2011; Thorstensen et al., 2011; Herz et al., 2013). So far, various HMTases have been characterized in animals and plants, primarily in somatic cells but rarely in germ cells. In Arabidopsis, several SET DOMAIN GROUP (SDG) proteins, including ATX1/SDG27, ATX2/SDG30, ATXR7/SDG25, and ATXR3/SDG2, have been reported to catalyze H3K4 methylation. Disruption of *ATX1* causes pleiotropic phenotypes, including homeotic transformation, root and leaf defects, and early flowering, whereas loss of *ATX2* alone does not have an obvious phenotype but can enhance *atx1* mutant defects (Alvarez-Venegas

et al., 2003; Pien et al., 2008; Saleh et al., 2008). The loss-of-function *sdg25/atxr7* mutant has an early flowering phenotype associated with suppression of *FLOWERING LOCUS C* expression (Berr et al., 2009; Tamada et al., 2009). Remarkably, *ATXR3/SDG2* is broadly expressed, and its disruption leads to severe and pleiotropic phenotypes, including dwarfism, short-root, impaired fertility, and altered circadian clock, as well as the misregulation of a large number of genes (Berr et al., 2010; Guo et al., 2010; Malapeira et al., 2012; Yun et al., 2012; Yao et al., 2013).

In this study, we investigate the function of SDG2 in chromatin reprogramming during male gametophyte development. While loss of *SDG2* does not show detectable effect on meiosis and cell fate acquisition, the loss-of-function *sdg2-1* mutant displays a pause or delay of developmental progression at bicellular pollen stage. Chromatin condensation was found elevated in the pollen vegetative cell nucleus, which is in association with a reduction of H3K4me3 and an ectopic speckle formation of the heterochromatin mark H3K9me2 detected in the *sdg2-1* pollen grains. Remarkably, in the *sdg2-1* mutant, the activation of retrotransposon *ATLANTYS1* in the pollen vegetative cell is impaired, and pollen germination as well as pollen tube elongation is inhibited. Our study thus establishes a crucial role of SDG2-mediated H3K4me3 in chromatin landscape regulation and postmeiotic microspore development and function.

RESULTS

Loss of SDG2 Barely Affects Male Meiosis

Arabidopsis *SDG2* has been shown to be essential in sporogenous tissues during specification of floral organs, as well as in gametophytic function (Berr et al., 2010; Guo et al., 2010). In these previous studies, several independent *sdg2* mutant alleles had been characterized to display similar loss-of-function mutant phenotype, and the mutant phenotype could be fully rescued to wild-type phenotype in complementation test. It was reported that independently from flower developmental defects, the probability of the *sdg2-1*, *sdg2-2*, or *sdg2-3* allele transmission from the selfing population in heterozygous (+/-) mutant plants is reduced roughly to 55 to 75%. Furthermore, analyses of reciprocal crosses between the control wild-type Columbia-0 (Col-0) and the heterozygous mutant *sdg2-1*(+/-) plants or between Col-0 and *sdg2-3*(+/-) plants showed that both male and female transmission are affected (Berr et al., 2010). The decreased transmission of mutant alleles does not result from an increase in embryo lethality (Berr et al., 2010). This phenotype might rather result from defects in meiosis progression and/or gametophyte development. To investigate those possibilities, we first monitored the different stages of meiosis in *sdg2-1* mutant using 4',6-diamino-phenylindole (DAPI) staining of microspore mother cells. Meiosis consists of two rounds of cell divisions after a single round of DNA replication, producing

haploid gametes. The meiosis events have been clearly described previously (Ross et al., 1996; Ma, 2005); the different meiotic stages observed in the control Col-0 plants are shown in Figure 1, A to J. During meiosis I in *sdg2-1*, the condensed homologous chromosomes form an array on the nuclear plate following synapsis and pairing in prophase I (Fig. 1, K–M), similarly as in Col-0 (Fig. 1, A–C). The homologous chromosomes then migrate to opposite poles in *sdg2-1* (Fig. 1, N and O) similarly as in Col-0 (Fig. 1, D and E), and after meiosis II, individual sister chromatids are separated to form tetrad of haploid nuclei in *sdg2-1* (Fig. 1, P to T) similarly as in Col-0 (Fig. 1, F–J). Based on the observation of more than 50 meiocytes at each meiotic stage, we found that the meiosis events in the *sdg2-1* mutant show no significant differences compared to Col-0. In conclusion, we could not detect any abnormal chromosome configuration during meiosis in *sdg2-1*, suggesting that *SDG2* activity rather regulates postmeiotic gametogenesis in Arabidopsis.

SDG2 Is Not Essential for Establishment of Pollen Vegetative and Sperm Cell Identity

To further characterize *SDG2* function during post-meiotic gametogenesis, we investigated the establishment of gametophytic cell fate in *sdg2-1* mutant. We analyzed postmeiotic events using specific vegetative and sperm cell nuclei reporters, respectively AC26-mRFP and HTR10-mRFP, combined with nuclear DAPI staining. The living-cell reporter HTR10-mRFP represents a fusion between the H3.3 variant HTR10 protein and the fluorescent protein mRFP under the control of the native *HTR10* promoter (Ingouff et al., 2007); and AC26-mRFP is associated with the expression of HISTONE H2B-mRFP fusion protein under the control of *ACTIN11* promoter (Rotman et al., 2005). Analyses under the confocal microscope revealed that HTR10-mRFP specifically marks the generative cell nucleus of bicellular pollen (Fig. 2A) and the two sperm cell nuclei of tricellular pollen (Fig. 2B) in a way similar

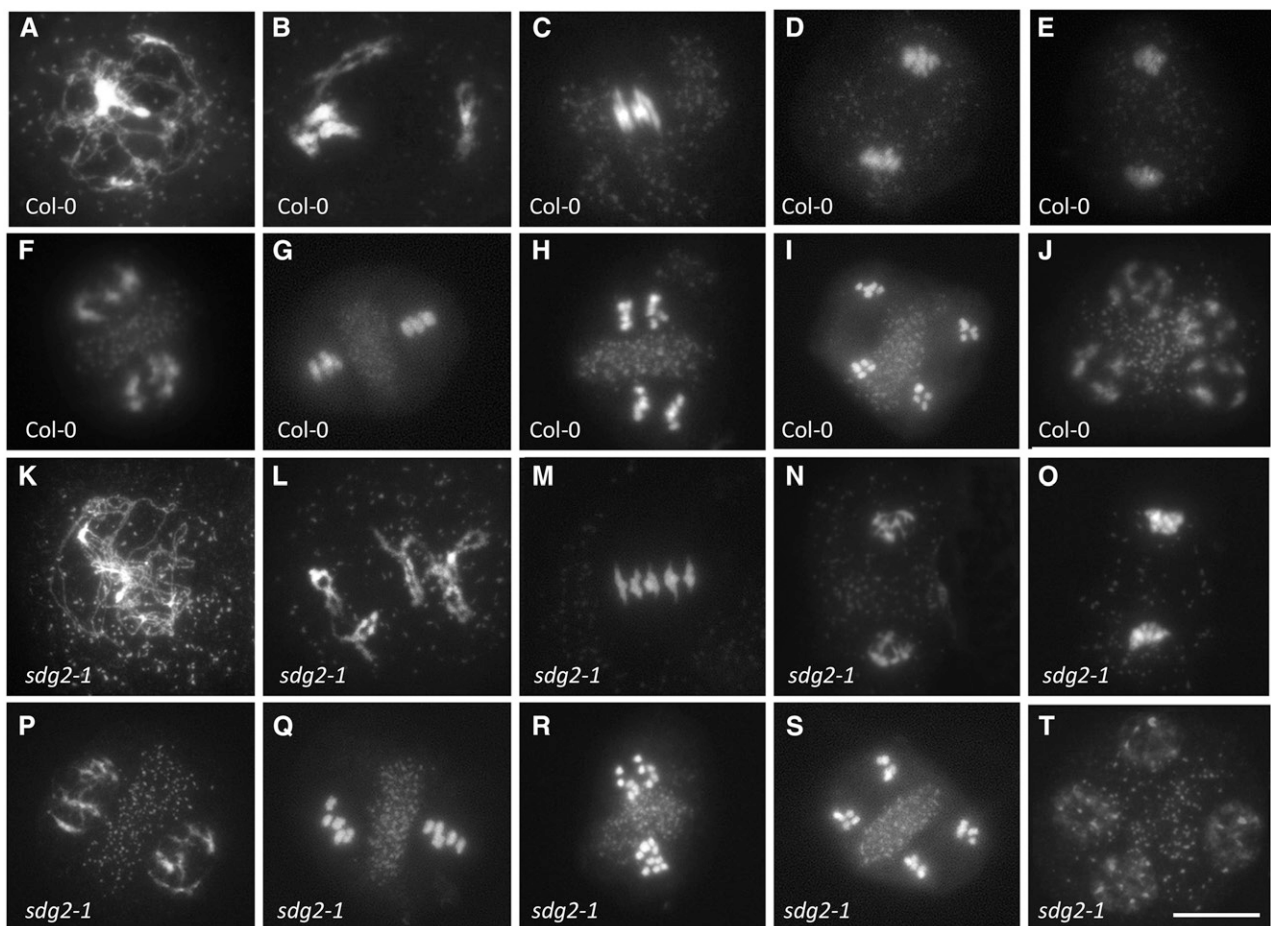


Figure 1. Male meiosis proceeds normally in the loss-of-function mutant *sdg2-1*. A to J, DAPI staining showing different stages of meiosis in the wild-type control Col-0. K to T, DAPI staining showing different stages of meiosis in *sdg2-1*. The shown stages correspond to zygotene (A and K), diakinesis (B and L), metaphase I (C and M), anaphase I (D and N), telophase I (E and O), interphase II (F and P), metaphase II (G and Q), anaphase II (H and R), telophase II (I and S), and newly formed tetrad (J and T). Scale bar = 10 μ m for all images.

to that between Col-0 and *sdg2-1*. Also, the vegetative cell marker AC26-mRFP was observed specifically marking the vegetative cell within the mature pollen in a way similar to that between Col-0 and *sdg2-1* (Fig. 2C). Our data thus indicate that the establishment of sperm and vegetative cell fate can occur normally in *sdg2-1* pollen. Furthermore, our observation also indicates that specific incorporation of the HTR10 variant before fertilization in the chromatin of generative and sperm cell nuclei (Ingouff et al., 2007) is unaffected in *sdg2-1*, compared to the wild type.

SDG2 Is Involved in the Timing of Pollen Development

To further understand *sdg2-1* pollen defects that lead to a reduced transmission of the mutant allele, we analyzed the developmental timing of pollen maturation. Anther formation in Arabidopsis is divided into 14 developmental stages (Sanders et al., 1999). The meiosis that will generate the microspores occurs around stage 6 of anther development. While the first mitotic division takes place at stage 11, the second division that will produce tricellular pollen is observed at anther developmental stage 12. We first examined bicellular stage pollen (anther stage 11) using HTR10-mRFP marker to count the number of generative/sperm nuclei per pollen. In both Col-0 and *sdg2-1*, more than 94% of pollen grains contained one generative nucleus per pollen as expected for normal development (Fig. 3A). Later, at development, in tricellular stage pollen (anther stages 12 and 13), 82% of the Col-0 pollen grains had two sperm nuclei per pollen marked with HTR10-mRFP, while only 65% of the *sdg2-1* pollen grains showed

two sperm nuclei per pollen, and 24% of the *sdg2-1* pollen grains showed one sperm nucleus per pollen (versus 11% in Col-0; Fig. 3B). To verify that *sdg2-1* pollen from anther stages 12 and 13 with one HTR10-mRFP positive nucleus is indeed at bicellular stage, we also used DAPI staining in examination. We found that *sdg2-1* pollen with one nucleus marked with HTR10-mRFP is always a bicellular pollen and never a tricellular pollen (Fig. 3C). Therefore, we conclude that the transition from bicellular to tricellular stage of pollen development is slowing down or paused in *sdg2-1*.

SDG2 Is Involved in Maintenance of Decondensed Chromatin State of Pollen Vegetative Cells

In both male and female gametophytes, specific cell types are characterized by specific chromatin organization. In wild-type Arabidopsis pollen, the vegetative cell nucleus contains a relatively decondensed chromatin, whereas the sperm nuclei contain highly condensed chromatin (Schoft et al., 2009). In *sdg2-1* mutant, global chromatin organization might be impaired, which would then affect pollen development. To verify this hypothesis, we analyzed DNA condensation in pollen vegetative and sperm cell nuclei using DAPI staining. Confocal analyses showed that at early stage of gametophyte development, DNA in haploid microspore is more condensed in *sdg2-1* than in Col-0 (Fig. 4A, top). At the following bicellular and tricellular stages of pollen development, we found that DNA condensation remained obviously higher in the vegetative cell nuclei of *sdg2-1* as compared to those of Col-0 (Fig. 4A, middle and bottom; Fig. 4, B and C). In

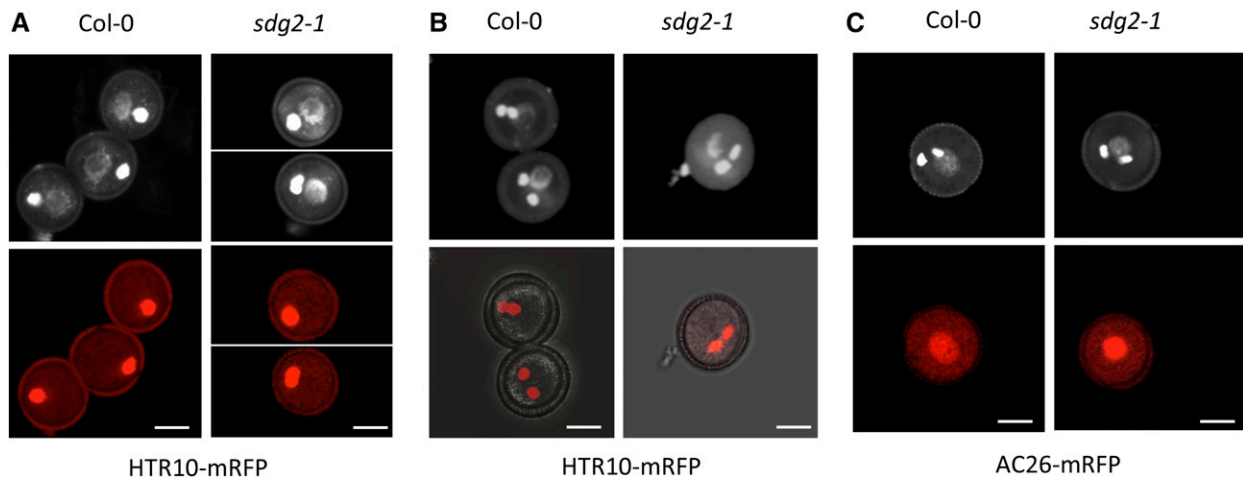


Figure 2. Male cell fate acquisition is unaffected in the loss-of-function mutant *sdg2-1*. A and B, DAPI (top) and HTR10-mRFP (bottom) fluorescent signals in pollen at bicellular and tricellular developmental stage, respectively. In B but not in A, the HTR10-mRFP fluorescence is shown together with its corresponding transmitted light reference image to visualize the entire mature pollen grain. Note for specific *HTR10-mRFP* expression in the generative (A) and sperm (B) cells within pollen grains in *sdg2-1* similarly as in the wild-type control Col-0. C, DAPI (top) and AC26-mRFP (bottom) fluorescent signals in tricellular stage pollen in Col-0 and *sdg2-1*. Note for specific AC26-mRFP signal detected in the vegetative cell nucleus but not in the sperm cells, similarly in *sdg2-1* and Col-0. Scale bars = 10 μ m for all images.

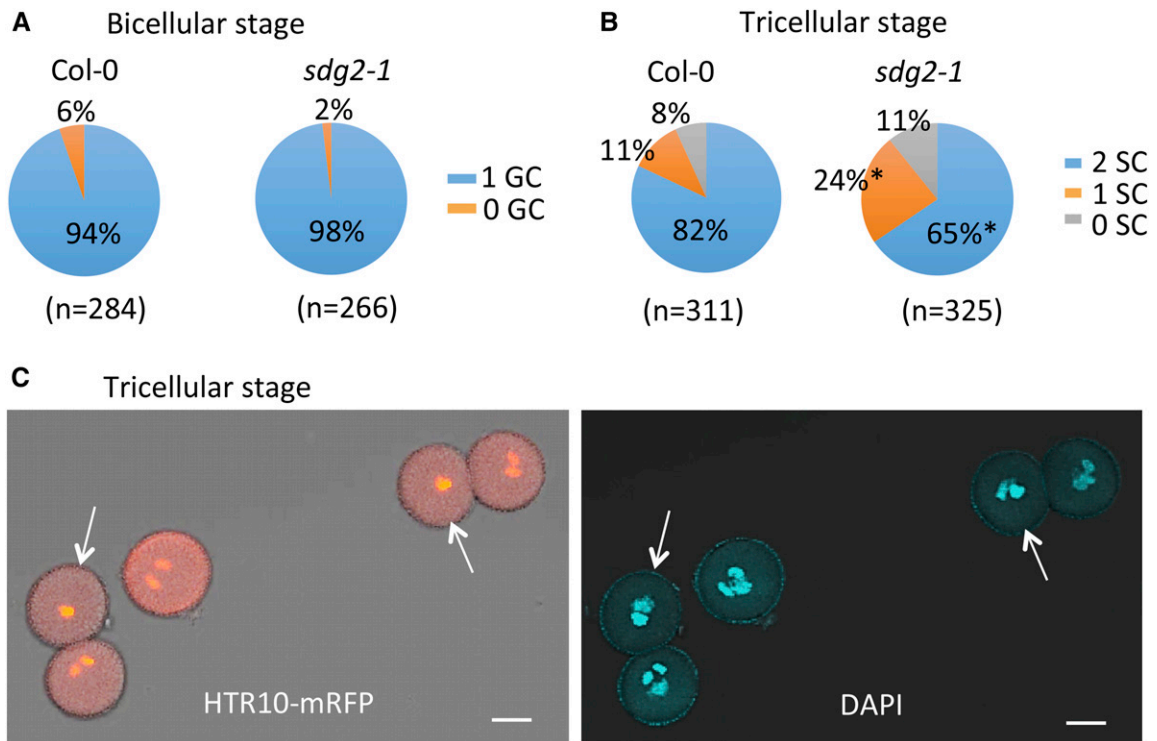


Figure 3. Loss of *SDG2* prevents mitotic division of pollen generative cell in the *sdg2-1* mutant. A, Graphic representation of pollen grains containing the indicated number of generative cells (GC) determined using HTR10-mRFP marker in *sdg2-1* and the wild-type control Col-0 at the bicellular pollen developmental stage. Pollen was examined from anthers at developmental stage 11 from over 10 individual plants for each genotype. The difference between *sdg2-1* and Col-0 is not significant according to unpaired *t* test ($P > 0.05$). B, Graphic representation of pollen grains containing the indicated number of sperm cells (SC) determined using HTR10-mRFP marker in *sdg2-1* and Col-0 at the tricellular pollen developmental stage. Pollen was examined from anthers at developmental stage 12 or 13 from over 10 individual plants for each genotype. Unpaired *t* test indicates that the difference between *sdg2-1* and Col-0 is statistically significant for 1 SC and 2 SC categories ($*P < 0.05$) but not for 0 SC category ($P > 0.05$). C, HTR10-mRFP (left) and DAPI (right) fluorescent signals in *sdg2-1* pollen grains at tricellular pollen developmental stage. Pollen was examined from anthers at developmental stage 12 or 13. Arrows indicate pollen grains arrested at bicellular stage without GC division. Scale bars = 10 μm .

contrast, significant differences in DNA condensation were undetectable in generative or sperm cell nuclei between *sdg2-1* and Col-0 (Fig. 4). Together, our data indicate that *SDG2* is required for proper chromatin decondensation in the microspore and later on in the vegetative cell nucleus at bicellular and tricellular stages of pollen development.

***SDG2*-Mediated H3K4me3 Prevents Ectopic Heterochromatic H3K9me2 Speckle Formation in Pollen Nuclei**

To confirm that *SDG2* is indeed involved in regulating H3K4me3 in pollen, we utilized anti-H3H4me3 antibodies to immunolocalize the histone mark in wild-type versus mutant pollen. We found that H3K4me3 is present in both vegetative and sperm nuclei of Col-0 pollen (Fig. 5A, top), and its signal intensity is greatly reduced in both vegetative and sperm nuclei of the *sdg2-1* mutant pollen (Fig. 5A, bottom) compared to Col-0 pollen (Fig. 5B). Western-blot analysis revealed that H3K4me3 level is

globally reduced in the *sdg2-1* inflorescence (Fig. 5C). These data are consistent with the previous reports showing that *SDG2* encodes a major H3K4-methyltransferase in Arabidopsis (Berr et al., 2010; Guo et al., 2010). In contrast to the euchromatin marker H3K4me3, H3K9me2 represents the heterochromatin marker in Arabidopsis. Our western-blot analysis failed to detect any clear changed level of H3K9me2 in the *sdg2-1* inflorescence (Fig. 5C). Our immunolocalization analysis showed that H3K9me2 is detected in speckles in the sperm cell nuclei but barely in the vegetative nucleus (<9%, $n = 56$) of Col-0 pollen (Fig. 5, D and E; Supplemental Fig. S1), which is in agreement with a previous study (Schoft et al., 2009). Interestingly, the *sdg2-1* mutant pollen showed clearly detectable H3K9me2 speckles in the vegetative nucleus (>30%, $n = 52$) as well as an increase of speckles in the sperm nuclei (Fig. 5, D and E; Supplemental Fig. S1). Examination of pollen at bicellular stage also revealed an increase of H3K9me2 speckles in both vegetative and generative nuclei in *sdg2-1* as compared to Col-0 (Fig. 5F; Supplemental Fig. S1). From those data, we conclude that

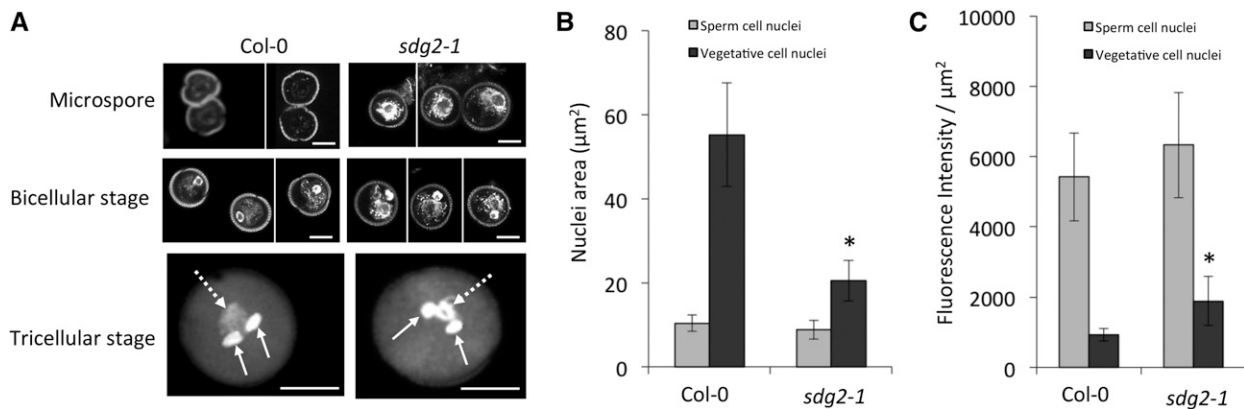


Figure 4. SDG2 is involved in promoting chromatin decondensation in microspore and in pollen vegetative cell nuclei. A, DAPI fluorescent signals in microspores and in pollen grains at the bicellular or tricellular stage in the wild-type control Col-0 and the loss-of-function mutant *sdg2-1*, as indicated. Note for more condensed chromatin in *sdg2-1* than in Col-0 in microspore and in the vegetative cell of bicellular or tricellular pollen. Dashed arrow indicates the vegetative cell nucleus, and solid arrows indicate sperm cells in the tricellular pollen. Scale bars = 10 µm. B, Graphic representation of the nuclei area from sperm cells and vegetative cells of mature tricellular stage pollen. The area was measured using ImageJ software from DAPI-staining microscopy images at the largest scan surface. C, Graphic representation of the DAPI fluorescence intensity per µm² from sperm and vegetative cell nuclei of mature tricellular stage pollen. The fluorescence intensity was measured using ImageJ software from the image scan displaying the brightest signal. Data shown in B and C represent mean together with error bar based on 40 pollen grains for each genotype per experiment from three independent experiments. The asterisk indicates where the difference between Col-0 and *sdg2-1* is significant in statistic test ($P < 0.05$).

SDG2-mediated H3K4me3 prevents ectopic heterochromatic H3K9me2 speckle formation, and that the reduced level of H3K4me3 together with H3K9me2 redistribution likely has caused high chromatin compaction observed in the vegetative nucleus of the *sdg2-1* mutant.

SDG2 Is Required for Active Expression of Retrotransposon *ATLANTYS1* in Pollen

Previous studies have revealed that global DNA demethylation specifically occurs in the pollen vegetative cell nucleus, and active transcription and production of mobile siRNAs from TEs in the vegetative cell are proposed to act on complementary TE silencing associated with compact chromatin in the sperm cell nuclei (Ibarra et al., 2012; Slotkin et al., 2009; Calarco et al., 2012). The presence of a more condensed DNA together with the decreased H3K4me3 in *sdg2-1* might affect TEs derepression in the pollen vegetative cell. To directly analyze the functional effect of chromatin condensation defect in *sdg2-1* pollen, we crossed *sdg2-1/+* with a GUS enhancer trap line ET5729, which contains an insertion of GUS coding sequence in an endogenous retrotransposon *ATLANTYS1* (Sundaresan et al., 1995; Slotkin et al., 2009). To eliminate possible mixed genetic background effect, we also crossed Col-0 with ET5729 (Landsberg *erecta* background) and used as control. GUS staining analysis revealed that wild-type Col-0 pollen is absent of staining (Fig. 6A), and pollen from F2 plants of Col-0 × ET5729 shows clear blue GUS staining (Fig. 6B). Interestingly, pollen from F2 plants of *sdg2-1* (Col-0 background) × ET5729 showed barely detectable GUS blue staining

(Fig. 6C). Consistently, at later generation, with the GUS reporter allele at a homozygous state, strong blue staining was detected in ET5729 (Col-0) control pollen (Fig. 6D), but not in ET5729 (*sdg2-1*) mutant pollen (Fig. 6E). Thus, our data indicate that *ATLANTYS1* activation is impaired in *sdg2-1*. Analysis of the previously published microarray data (Berr et al., 2010) revealed that 20 TE genes are down-regulated by more than 2-fold in *sdg2-1* compared to Col-0 flower buds (Supplemental Table S1). Transcripts of the majority of these TE genes are detectable in the male meiocyte (Yang et al., 2011) and/or in pollen (Loraine et al., 2013) by RNA sequencing (RNA-seq) analysis. More notably, among these TE genes At5g28626 corresponds to a full-length *SADHU* element, which is disrupted by an *ATLANTYS2*-like retrotransposon LTR sequence and controlled in silencing by DNA methylation in some Arabidopsis accessions (Rangwala et al., 2006). Collectively, the data indicate that transcription activation of various TE genes relies on SDG2, which is in agreement with the reduced H3K4me3 and high chromatin compaction observed in the vegetative cell of *sdg2-1* pollen.

SDG2 Plays a Critical Role in Pollen Germination and Pollen Tube Elongation

A major function of pollen vegetative cell activity is to assure pollen germination and subsequent pollen tube elongation to deliver sperm cells for fertilization. Lastly, we addressed the question of whether SDG2 plays a role in these processes. Thus, we carried out in vitro pollen germination assays. After 8 h incubation on appropriate culture medium, nearly 77% of the Col-0

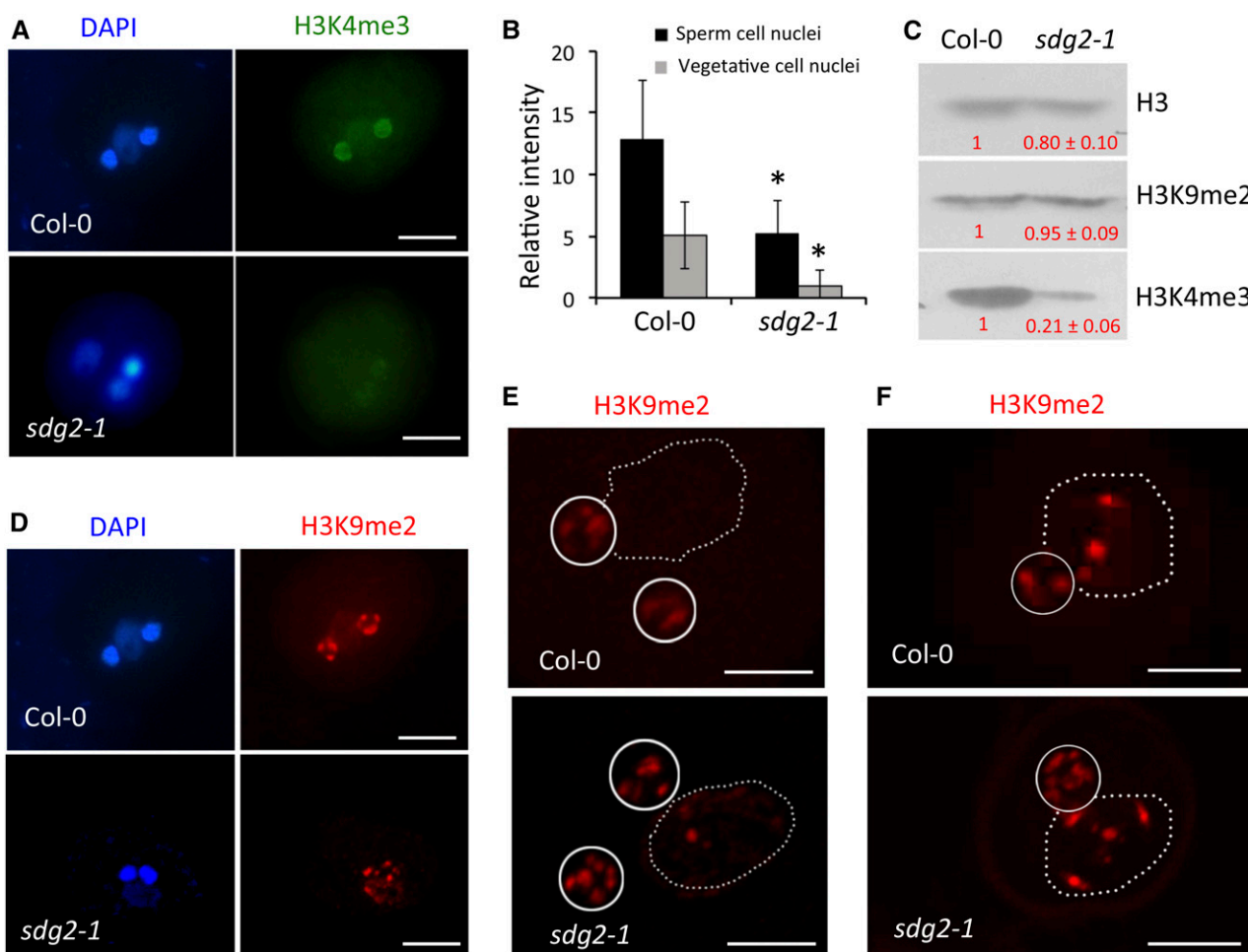


Figure 5. *SDG2* contributes to H3K4me3 and H3K9me2 patterning in pollen. **A**, Immunofluorescence staining performed with anti-H3K4me3 antibody in tricellular pollen in the wild-type control Col-0 (top) and the *sdg2-1* mutant (bottom). DAPI staining of the same pollen is shown on left. Note for drastically reduced H3K4me3 signal in the vegetative cell nucleus and the two sperm nuclei of the *sdg2-1* pollen as compared to the Col-0 pollen. **B**, Graphic representation of the relative H3K4me3 fluorescence intensity, after normalization using DAPI, in sperm cell and vegetative cell nuclei of Col-0 and *sdg2-1* (set as 1 for *sdg2-1* vegetative cell nuclei). The fluorescence intensity was measured using ImageJ software, and mean values from 10 pollen grains are shown together with error bars. The asterisk indicates where the difference between Col-0 and *sdg2-1* is significant in statistic test ($P < 0.05$). **C**, Western-blot analysis of H3K4me3 and H3K9me2 levels in *sdg2-1*. Histone-enriched proteins were extracted from inflorescence of Col-0 and *sdg2-1* plants grown under a 16 h light/8 h dark photoperiod. H3K9me2, H3K4me3, and total H3 proteins were detected using specific antibodies. Numbers indicate mean (\pm SE) of relative densitometry values measured from three independent experiments, in *sdg2-1* and Col-0 (set as 1). **D**, Immunofluorescence staining performed with anti-H3K9me2 antibody in tricellular pollen in Col-0 (top) and *sdg2-1* (bottom). DAPI staining of the same pollen is shown on left. Note for H3K9me2, speckles detected in the *sdg2-1* pollen vegetative cell nucleus, but not in the Col-0 pollen vegetative cell nucleus. **E**, Close-up images showing H3K9me2 speckles in the *sdg2-1*, but not in the Col-0 pollen vegetative nucleus (dashed circle) as well as in the sperm nuclei (circles) of both *sdg2-1* and Col-0 pollen. **F**, Images showing H3K9me2 speckles in the vegetative nucleus (dashed circle) and in the generative nucleus (circles) of bicellular pollen in Col-0 and *sdg2-1*. Scale bars = 10 μ m for A and D and 5 μ m for E and F.

pollen grains produced pollen tubes ($n = 300$), while the germination ratio of the *sdg2-1* mutant pollen grains arrived only to about 10% ($n = 300$; Fig. 6, F and G). Moreover, the length of the mutant pollen tube was drastically inhibited, as compared to the good length of wild-type pollen tube (Fig. 6F). These data clearly demonstrate that loss of *SDG2* impairs pollen germination and pollen tube elongation, which is in line with high chromatin compaction and compromised

transcription activity observed in the *sdg2-1* pollen vegetative cell.

DISCUSSION

In this study, we show that *SDG2*-mediated H3K4me3 participates in the epigenetic reprogramming observed during Arabidopsis male gametogenesis. Although male meiosis and cell fate acquisition can occur normally in

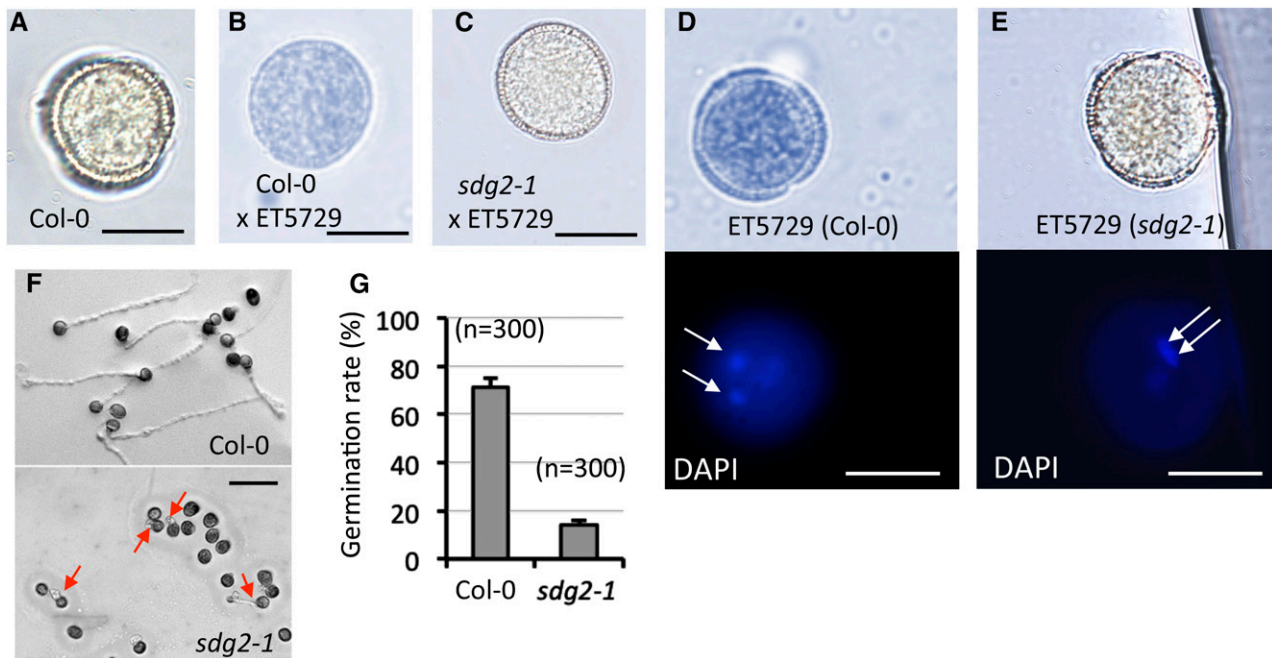


Figure 6. SDG2 is involved in activation of retransposon *ATLANTYS1* transcription and in promoting pollen germination and pollen tube growth. A to C, GUS staining of tricellular stage pollen in bright field microscopy from Col-0 (A), from a F2 plant generated by the cross between the wild-type control Col-0 and the enhancer trap line ET5729 (B), or between *sdg2-1* and ET5729 (C). D and E, GUS staining of tricellular stage pollen from plants homozygous for ET5729 in, respectively, Col-0 (D) and *sdg2-1* (E) backgrounds. Bottom, the corresponding DAPI stained pollen. Arrows indicate the sperm cell nuclei. F, Representative images showing in vitro germination of pollen from Col-0 and *sdg2-1*. Red arrows indicate germinated *sdg2-1* pollen but with pollen tube elongation inhibited. G, Graphic representation of *sdg2-1* and Col-0 pollen germination rate. Scale bars = 10 μm for A to E and 200 μm for F.

the *sdg2-1* mutant, SDG2-mediated H3K4me3 is crucial in promoting postmeiotic microspore chromatin decondensation, mitotic cell division, and activation of retrotransposon *ATLANTYS1*. Consistent with a compromised vegetative cell function, pollen germination and pollen tube elongation are found inhibited in the *sdg2-1* mutant.

In wild-type Arabidopsis, as compared to surrounding somatic cells, both megaspore and microspore mother cells display more decondensed chromatin with higher levels of H3K4me2 and H3K4me3 (She et al., 2013; She and Baroux, 2015). The *MALE MEIOCYTE DEATH1* (*MMD1*, also known as *DUET*) gene encodes a PHD-finger protein essential for male meiosis (Reddy et al., 2003; Yang et al., 2003). Loss of *MMD1/DUET* function causes multiple defects, including cytoplasmic collapse and cell death of meiocytes with possible DNA fragmentation, delay in progression and arrest at metaphase I, and formation of aberrant meiotic products such as dyads and triads (Reddy et al., 2003; Yang et al., 2003; Andreuzza et al., 2015). More recent studies demonstrate that the *MMD1/DUET* PHD-finger exhibits binding activities to modified histone H3 peptides including H3K4me2 and H3K4me3 and that its mutation compromises *MMD1/DUET* biological function (Andreuzza et al., 2015; Wang et al., 2016). Based on these previous studies, one can predict that H3K4me2/me3 might play crucial roles in Arabidopsis

male meiosis. In contrast, however, depletion of the Arabidopsis major H3K4me2/me3-methyltransferase SDG2 in the *sdg2-1* mutant (Berr et al., 2010; Guo et al., 2010) showed normal male meiosis without any detectable chromosomal abnormality throughout different meiotic phases (Fig. 1). The female meiosis also occurs normally in the *sdg2-1* mutant, albeit reduced H3K4me3 in megaspore mother cells (She et al., 2013). It seems that Arabidopsis meiosis is rather tolerant to H3K4me3 reduction. Nevertheless, cautions are necessary because Arabidopsis contains multiple H3K4-methyltransferases that may have overlapping/redundant function in meiosis. Transcripts of *SDG2* as well as those of *ATX1*, *ATX2*, and *SDG4* have been detected in male meiocytes (Yang et al., 2011). Moreover, *SDG4* has been reported to contribute to pollen function, likely through methylation of H3K4 and H3K36 (Cartagena et al., 2008). Future studies will be required to verify possible overlapping/redundant functions of these different HMTase genes to better understand the role of H3K4me2/me3 deposition in Arabidopsis meiosis.

After meiosis II, sister chromatids are separated to form tetrads of haploid cells in *sdg2-1* as in Col-0 (Fig. 1, P and T). Nevertheless, tetrad analysis has revealed significant loss of nuclei in *sdg2-1* (Berr et al., 2010), indicating that chromatin in the mutant might be unstable and DNA degradation might have occurred in some mutant microspores. During gametogenesis, the

first haploid cell division leads to establishment of the vegetative cell and the generative cell at bicellular pollen stage, and the second mitotic cell division occurs specifically from the generative cell, resulting in tricellular pollen containing the vegetative cell and two sperm cells. Our analysis of living pollen grains shows that cell fate acquisition can occur normally in the *sdg2-1* mutant (Fig. 2). However, *SDG2*-depletion prevents the second pollen mitosis, generating a fraction of pollen grains comprising a vegetative cell and a single sperm cell (Fig. 3). One major regulator of sperm cell identity and cell cycle progression is the transcription factor *DUO POLLEN1* (*DUO1*; Rotman et al., 2005; Borg et al., 2011, 2014). In the loss-of-function mutant *duo1*, the generative cell fails to divide to generate two sperm cells, and the mutant pollen cannot fertilize the female egg cell or central cell. Specific expression of the histone variant gene *HTR10* in sperm cells is under the direct control of *DUO1* (Borg et al., 2014). Our study shows that *HTR10-mRFP* expression is unaffected in the *sdg2-1* pollen (Figs. 2 and 3), suggesting that *SDG2* acts independently from the *DUO1* pathway. The more condensed chromatin observed in the vegetative cell (Fig. 4) might have affected its genome function and indirectly impaired generative cell division in the *sdg2-1* pollen. The histone chaperone *CHROMATIN ASSEMBLY FACTOR1*, which is involved in de novo assembly of nucleosomes in a replication-dependent manner, is also required for mitotic cell division, but not for cell fate maintenance during pollen development (Chen et al., 2008). Together, those data suggest the existence of a strong link between the chromatin landscape and cell cycle progression for proper pollen development.

Highly condensed chromatin of sperm cells is thought to serve as a mechanism to ensure genome integrity, e.g. by suppression of TE transposition because uncontrolled TE transposition could cause insertions, deletions, and/or other rearrangements of the genome (Slotkin et al., 2009). Distinct from sperm cells, the pollen vegetative cell does not transfer its genomic DNA to the fertilization products during plant reproduction. The less-condensed chromatin allows active TE transcription, and production of mobile siRNAs from TEs in the pollen vegetative cell has been proposed to move to promote TE silencing associated with DNA methylation in the pollen sperm cell nuclei (Ibarra et al., 2012; Slotkin et al., 2009; Calarco et al., 2012). Genome-wide analysis using Arabidopsis seedlings reveals that H3K4me2/3 and DNA methylation are mutually exclusive (Zhang et al., 2009). The *sdg2-1* mutant has reduced H3K4me3 levels and its pollen vegetative cell exhibits more condensed chromatin (Figs. 4 and 5). Consistent with the role of H3K4me3 in promoting euchromatinization and transcription activation, expression of the retrotransposon *ATLANTYS1* and likely also some other TE genes is impaired in the *sdg2-1* pollen (Fig. 6; Supplemental Table S1). Remarkably, the *sdg2-1* pollen nuclei display ectopic speckles of H3K9me2, the main histone modification associated with DNA methylation in heterochromatinization in somatic tissues of Arabidopsis

(Stroud et al., 2013). It is currently unknown whether H3K9me2 heterochromatinization is associated with TE silencing and/or whether the H3K4me3 reduction directly or indirectly causes the impaired TE expression in the *sdg2-1* mutant pollen.

In wild-type Arabidopsis pollen, H3K4me3 is found in both the vegetative cell nucleus and the sperm nuclei, whereas H3K9me2 is present specifically in the sperm cell nuclei (Fig. 5; Schoft et al., 2009). Remarkably, a recent study demonstrates that H3K4me3 is present at similar levels in vegetative, generative, and sperm nuclear extracts of lily (*Lilium davidii*) pollen, whereas H3K9me2 and H3K9me3 are detected at higher levels in vegetative than in generative or sperm nuclear extract (Yang et al., 2016). Thus, pollen cell-type-specific pattern of H3K9me2 accumulation is likely plant species dependent. Nevertheless, H3K9me2 in the lily (*Lilium longiflorum*) pollen vegetative cell nucleus is colocalized with DAPI-staining regions (Sano and Tanaka, 2010), indicating that the heterochromatic nature of H3K9me2 remains similar in lily as in Arabidopsis. Our study showed that, albeit reduced H3K4me3, chromatin compaction remains largely unaffected in the *sdg2-1* pollen sperm nuclei. It becomes evident that future studies are required to further investigate histone methylation function in chromatin condensation in pollen sperm cells. Distinctively, our data clearly establish a crucial function of H3K4me3 deposition in the pollen vegetative cell. *SDG2*-dependent H3K4me3 deficiency prevents pollen germination and pollen tube elongation. Chromatin landscape seems to be tightly associated with the active transcriptional genome program of the pollen vegetative cell, which is key for pollen tube growth to guide the delivery of sperm cells to the ovule for fertilization.

MATERIALS AND METHODS

Plant Material

sdg2-1 mutant has been described previously (Berr et al., 2010). Seeds from the reporters AC26-mRFP and HTR10-mRFP were kindly provided by Frederic Berger (Chen et al., 2008). *sdg2-1* mutant and the two reporter lines mentioned previously are in the Col-0 background. Both reporter lines were crossed with *sdg2-1/+*. Plants homozygous for the fluorescent marker and heterozygous for *sdg2-1/+* were selected in F2 population by analyzing RFP segregation in mature pollen and PCR-based genotyping (Berr et al., 2010) to identify *sdg2-1* allele. Then F3 plants homozygous for both the fluorescent reporter and *sdg2-1* were identified based on *sdg2-1* phenotype (Berr et al., 2010). The GUS enhancer trap line ET5729 was kindly provided by Mathieu Ingouff. ET5729 is in the Landsberg *erecta* background and was crossed to wild-type Col-0 plants (controls) and *sdg2-1/+* plants to generate in F3 progeny plants homozygous for *sdg2-1* and ET5729. Seedlings (until 1 week old) were grown at 21°C to 22°C under continuous white light and on Murashige and Skoog medium supplemented with 0.8% of plant agar (Sigma-Aldrich). Then seedlings were transferred on standard potting soil at 21°C to 22°C under a 12-h-light/12-h-dark cycle for 3 weeks and then to a photoperiod of 16 h light/8 h dark.

Chromosome Spreading Analysis and Immunostaining

Microspores from all stages of meiosis were collected from fresh floral buds, fixed in Carnoy's fixative solution (ethanol:chloroform:acetic acid = 6:3:1), prepared for chromosome spreads as described previously (Ross et al., 1996), and stained with DAPI (0.1 µg/mL). Immunostainings of histone modifications were performed on bicellular and tricellular pollen collected after anther

dissection from floral stages 10 to 12. The collected pollens were fixed in 4% paraformaldehyde in PBS for 30 min and then kept in 1% Suc solution overnight at 4°C. After washing, the samples were incubated with the anti-H3K4me3 antibody (Millipore) or the anti-H3K9me2 antibody (Millipore) at 1:200 dilution. Alexa Fluor 488-conjugated anti-rabbit IgG antibodies (Invitrogen) and 594-conjugated anti-mouse IgG antibodies (Invitrogen) were used specifically as the secondary antibody.

Microscopy

DAPI staining of pollen grains was performed according to a previous report (Park et al., 1998). Epifluorescent images (mRFP-fusion proteins and DAPI-stained DNA) were acquired using Zeiss Imager A2 microscope (Figs. 1 and 5) and Zeiss LSM710 confocal laser-scanning microscopy (Figs. 2–4 and 6). GUS staining was performed following the protocol described previously (Johnson et al., 2004). Here, pollen grains were incubated with X-Gluc overnight at 37°C and imaged under a phase-contrast microscope.

Histone Extraction and Western-Blot Analysis

Histone-enriched proteins were extracted from inflorescence according a previously described method (Yu et al., 2004). Western-blot assays were performed to detect the covalent modification status of H3 tails (Yu et al., 2004). Antibodies against histone H3K4me3, H3K9me2, and H3 (Millipore) were used at 1:2,000 dilution.

Quantification and Statistical Analysis

Densitometry quantification of western blots and fluorescent intensity quantification of microscopy images were performed by using ImageJ software (<https://imagej.nih.gov/ij/>). For each pollen grain, confocal image with maximum fluorescence intensity was used in measurement at individual nucleus level, divided by nuclear area size, and normalized using a similar size area in the cytoplasm as background. Statistical analysis was performed by unpaired *t* test using GraphPad InStat v. 3.05 (GraphPad Software; <http://www.graphpad.com>).

In Vitro Pollen Germination Assay

In vitro pollen tube growth assay was performed as described previously (Li et al., 1999). Briefly, pollen grains from dehiscent anthers were carefully plated onto the surface of agar plates. The plates were then immediately transferred to a chamber at 25°C and 100% relative humidity. Pollen grains were cultured for 8 h, and the germination ratio was calculated by counting 300 pollen grains under a light microscope. This experiment was repeated three times with three plates per repeat.

Supplemental Data

The following supplemental materials are available.

Supplemental Figure S1. Immunofluorescence-staining analysis of the wild-type control Col-0 and the *sdg2-1* mutant pollen.

Supplemental Table S1. List of transposable element genes down-regulated by more than 2-fold *sdg2-1* compared to wild-type flower buds.

ACKNOWLEDGMENTS

We thank Zhihao Cheng for technical assistance in chromosome spreading experiments, and Hongxing Yang, Yingxiang Wang, and Hong Ma for providing male meicyote transcriptome data and helpful discussions.

Received March 3, 2017; accepted April 25, 2017; published April 28, 2017.

LITERATURE CITED

Alvarez-Venegas R, Pien S, Sadler M, Witmer X, Grossniklaus U, Avramova Z (2003) ATX-1, an Arabidopsis homolog of trithorax, activates flower homeotic genes. *Curr Biol* **13**: 627–637

- Andreuzza S, Nishal B, Singh A, Siddiqi I (2015) The chromatin protein DUET/MMD1 controls expression of the meiotic gene TDM1 during male meiosis in Arabidopsis. *PLoS Genet* **11**: e1005396
- Berger F, Twell D (2011) Germline specification and function in plants. *Annu Rev Plant Biol* **62**: 461–484
- Berr A, McCallum EJ, Ménard R, Meyer D, Fuchs J, Dong A, Shen WH (2010) Arabidopsis SET DOMAIN GROUP2 is required for H3K4 trimethylation and is crucial for both sporophyte and gametophyte development. *Plant Cell* **22**: 3232–3248
- Berr A, Xu L, Gao J, Cognat V, Steinmetz A, Dong A, Shen WH (2009) SET DOMAIN GROUP25 encodes a histone methyltransferase and is involved in FLOWERING LOCUS C activation and repression of flowering. *Plant Physiol* **151**: 1476–1485
- Borg M, Brownfield L, Khatib H, Sidorova A, Lingaya M, Twell D (2011) The R2R3 MYB transcription factor DUO1 activates a male germline-specific regulon essential for sperm cell differentiation in Arabidopsis. *Plant Cell* **23**: 534–549
- Borg M, Rutley N, Kagale S, Hamamura Y, Gherghinoiu M, Kumar S, Sari U, Esparza-Franco MA, Sakamoto W, Rozwadowski K, et al (2014) An EAR-dependent regulatory module promotes male germ cell division and sperm fertility in Arabidopsis. *Plant Cell* **26**: 2098–2113
- Calarco JP, Borges F, Donoghue MT, Van Ex F, Jullien PE, Lopes T, Gardner R, Berger F, Feijó JA, Becker JD, et al (2012) Reprogramming of DNA methylation in pollen guides epigenetic inheritance via small RNA. *Cell* **151**: 194–205
- Cartagena JA, Matsunaga S, Seki M, Kurihara D, Yokoyama M, Shinozaki K, Fujimoto S, Azumi Y, Uchiyama S, Fukui K (2008) The Arabidopsis SDG4 contributes to the regulation of pollen tube growth by methylation of histone H3 lysines 4 and 36 in mature pollen. *Dev Biol* **315**: 355–368
- Chen Z, Tan JL, Ingouff M, Sundaresan V, Berger F (2008) Chromatin assembly factor 1 regulates the cell cycle but not cell fate during male gametogenesis in *Arabidopsis thaliana*. *Development* **135**: 65–73
- Feng S, Jacobsen SE, Reik W (2010) Epigenetic reprogramming in plant and animal development. *Science* **330**: 622–627
- Guo L, Yu Y, Law JA, Zhang X (2010) SET DOMAIN GROUP2 is the major histone H3 lysine [corrected] 4 trimethyltransferase in Arabidopsis. *Proc Natl Acad Sci USA* **107**: 18557–18562
- Hamamura Y, Nagahara S, Higashiyama T (2012) Double fertilization on the move. *Curr Opin Plant Biol* **15**: 70–77
- Herz HM, Garruss A, Shilatifard A (2013) SET for life: Biochemical activities and biological functions of SET domain-containing proteins. *Trends Biochem Sci* **38**: 621–639
- Houben A, Kumke K, Nagaki K, Hause G (2011) CENH3 distribution and differential chromatin modifications during pollen development in rye (*Secale cereale* L.). *Chromosome Res* **19**: 471–480
- Huang Y, Liu C, Shen WH, Ruan Y (2011) Phylogenetic analysis and classification of the *Brassica rapa* SET-domain protein family. *BMC Plant Biol* **11**: 175
- Ibarra CA, Feng X, Schoft VK, Hsieh TF, Uzawa R, Rodrigues JA, Zemach A, Chumak N, Machlicova A, Nishimura T, et al (2012) Active DNA demethylation in plant companion cells reinforces transposon methylation in gametes. *Science* **337**: 1360–1364
- Ingouff M, Hamamura Y, Gourgues M, Higashiyama T, Berger F (2007) Distinct dynamics of HISTONE3 variants between the two fertilization products in plants. *Curr Biol* **17**: 1032–1037
- Ingouff M, Rademacher S, Holec S, Soljić L, Xin N, Readshaw A, Foo SH, Lahouze B, Sprunck S, Berger F (2010) Zygotic resetting of the HISTONE 3 variant repertoire participates in epigenetic reprogramming in Arabidopsis. *Curr Biol* **20**: 2137–2143
- Ingouff M, Selles B, Michaud C, Vu TM, Berger F, Schorn AJ, Autran D, Van Durme M, Nowack MK, Martienssen RA, et al (2017) Live-cell analysis of DNA methylation during sexual reproduction in Arabidopsis reveals context and sex-specific dynamics controlled by non-canonical RdDM. *Genes Dev* **31**: 72–83
- Johnson MA, von Besser K, Zhou Q, Smith E, Aux G, Patton D, Levin JZ, Preuss D (2004) Arabidopsis hapless mutations define essential gametophytic functions. *Genetics* **168**: 971–982
- Jullien PE, Susaki D, Yelagandula R, Higashiyama T, Berger F (2012) DNA methylation dynamics during sexual reproduction in *Arabidopsis thaliana*. *Curr Biol* **22**: 1825–1830
- Kawashima T, Berger F (2014) Epigenetic reprogramming in plant sexual reproduction. *Nat Rev Genet* **15**: 613–624

- Lesch BJ, Page DC** (2014) Poised chromatin in the mammalian germ line. *Development* **141**: 3619–3626
- Li H, Lin Y, Heath RM, Zhu MX, Yang Z** (1999) Control of pollen tube tip growth by a Rop GTPase-dependent pathway that leads to tip-localized calcium influx. *Plant Cell* **11**: 1731–1742
- Loraine AE, McCormick S, Estrada A, Patel K, Qin P** (2013) RNA-seq of *Arabidopsis* pollen uncovers novel transcription and alternative splicing. *Plant Physiol* **162**: 1092–1109
- Ma H** (2005) Molecular genetic analyses of microsporogenesis and microgametogenesis in flowering plants. *Annu Rev Plant Biol* **56**: 393–434
- Malapeira J, Khaitova LC, Mas P** (2012) Ordered changes in histone modifications at the core of the *Arabidopsis* circadian clock. *Proc Natl Acad Sci USA* **109**: 21540–21545
- Ooi SL, Henikoff S** (2007) Germline histone dynamics and epigenetics. *Curr Opin Cell Biol* **19**: 257–265
- Pandey P, Houben A, Kumlehn J, Melzer M, Rutten T** (2013) Chromatin alterations during pollen development in *Hordeum vulgare*. *Cytogenet Genome Res* **141**: 50–57
- Park SK, Howden R, Twell D** (1998) The *Arabidopsis thaliana* gametophytic mutation gemini pollen1 disrupts microspore polarity, division asymmetry and pollen cell fate. *Development* **125**: 3789–3799
- Pien S, Fleury D, Mylne JS, Crevillen P, Inzé D, Avramova Z, Dean C, Grossniklaus U** (2008) ARABIDOPSIS TRITHORAX1 dynamically regulates FLOWERING LOCUS C activation via histone 3 lysine 4 trimethylation. *Plant Cell* **20**: 580–588
- Rangwala SH, Elumalai R, Vanier C, Ozkan H, Galbraith DW, Richards EJ** (2006) Meiotically stable natural epialleles of Sadhu, a novel *Arabidopsis* retroposon. *PLoS Genet* **2**: e36
- Reddy TV, Kaur J, Agashe B, Sundaresan V, Siddiqi I** (2003) The DUET gene is necessary for chromosome organization and progression during male meiosis in *Arabidopsis* and encodes a PHD finger protein. *Development* **130**: 5975–5987
- Ross KJ, Franz P, Jones GH** (1996) A light microscopic atlas of meiosis in *Arabidopsis thaliana*. *Chromosome Res* **4**: 507–516
- Rotman N, Durberry A, Wardle A, Yang WC, Chaboud A, Faure JE, Berger F, Twell D** (2005) A novel class of MYB factors controls sperm-cell formation in plants. *Curr Biol* **15**: 244–248
- Saitou M, Kurimoto K** (2014) Paternal nucleosomes: Are they retained in developmental promoters or gene deserts? *Dev Cell* **30**: 6–8
- Saleh A, Alvarez-Venegas R, Yilmaz M, Le O, Hou G, Sadler M, Al-Abdallat A, Xia Y, Lu G, Ladunga I, et al** (2008) The highly similar *Arabidopsis* homologs of trithorax ATX1 and ATX2 encode proteins with divergent biochemical functions. *Plant Cell* **20**: 568–579
- Sanders PM, Bui AQ, Weterings K, McIntire KN, Hsu Y-C, Lee PY, Truong MT, Beals TP, Goldberg RB** (1999) Anther developmental defects in *Arabidopsis thaliana* male-sterile mutants. *Sex Plant Reprod* **11**: 26
- Sano Y, Tanaka I** (2010) Distinct localization of histone H3 methylation in the vegetative nucleus of lily pollen. *Cell Biol Int* **34**: 253–259
- Sasaki H, Matsui Y** (2008) Epigenetic events in mammalian germ-cell development: Reprogramming and beyond. *Nat Rev Genet* **9**: 129–140
- Saze H, Mittelsten Scheid O, Paszkowski J** (2003) Maintenance of CpG methylation is essential for epigenetic inheritance during plant gametogenesis. *Nat Genet* **34**: 65–69
- Schmid MW, Schmidt A, Grossniklaus U** (2015) The female gametophyte: An emerging model for cell type-specific systems biology in plant development. *Front Plant Sci* **6**: 907
- Schoft VK, Chumak N, Mosiolek M, Slusarz L, Komnenovic V, Brownfield L, Twell D, Kakutani T, Tamaru H** (2009) Induction of RNA-directed DNA methylation upon decondensation of constitutive heterochromatin. *EMBO Rep* **10**: 1015–1021
- She W, Baroux C** (2015) Chromatin dynamics in pollen mother cells underpin a common scenario at the somatic-to-reproductive fate transition of both the male and female lineages in *Arabidopsis*. *Front Plant Sci* **6**: 294
- She W, Grimanelli D, Rutowicz K, Whitehead MW, Puzio M, Kotlinski M, Jerzmanowski A, Baroux C** (2013) Chromatin reprogramming during the somatic-to-reproductive cell fate transition in plants. *Development* **140**: 4008–4019
- Slotkin RK, Vaughn M, Borges F, Tanurdzić M, Becker JD, Feijó JA, Martienssen RA** (2009) Epigenetic reprogramming and small RNA silencing of transposable elements in pollen. *Cell* **136**: 461–472
- Stroud H, Greenberg MV, Feng S, Bernatavichute YV, Jacobsen SE** (2013) Comprehensive analysis of silencing mutants reveals complex regulation of the *Arabidopsis* methylome. *Cell* **152**: 352–364
- Sundaresan V, Springer P, Volpe T, Haward S, Jones JD, Dean C, Ma H, Martienssen R** (1995) Patterns of gene action in plant development revealed by enhancer trap and gene trap transposable elements. *Genes Dev* **9**: 1797–1810
- Tamada Y, Yun JY, Woo SC, Amasino RM** (2009) ARABIDOPSIS TRITHORAX-RELATED7 is required for methylation of lysine 4 of histone H3 and for transcriptional activation of FLOWERING LOCUS C. *Plant Cell* **21**: 3257–3269
- Thorntensen T, Grini PE, Aalen RB** (2011) SET domain proteins in plant development. *Biochim Biophys Acta* **1809**: 407–420
- Wang J, Niu B, Huang J, Wang H, Yang X, Dong A, Makaroff C, Ma H, Wang Y** (2016) The PHD finger protein MMD1/DUET ensures the progression of male meiotic chromosome condensation and directly regulates the expression of the condensin gene CAP-D3. *Plant Cell* **28**: 1894–1909
- Yang H, Lu P, Wang Y, Ma H** (2011) The transcriptome landscape of *Arabidopsis* male meiocytes from high-throughput sequencing: The complexity and evolution of the meiotic process. *Plant J* **65**: 503–516
- Yang X, Makaroff CA, Ma H** (2003) The *Arabidopsis* MALE MEIOCYTE DEATH1 gene encodes a PHD-finger protein that is required for male meiosis. *Plant Cell* **15**: 1281–1295
- Yang H, Yang N, Wang T** (2016) Proteomic analysis reveals the differential histone programs between male germline cells and vegetative cells in *Lilium davidii*. *Plant J* **85**: 660–674
- Yao X, Feng H, Yu Y, Dong A, Shen WH** (2013) SDG2-mediated H3K4 methylation is required for proper *Arabidopsis* root growth and development. *PLoS One* **8**: e56537
- Yu Y, Dong A, Shen WH** (2004) Molecular characterization of the tobacco SET domain protein NtSET1 unravels its role in histone methylation, chromatin binding, and segregation. *Plant J* **40**: 699–711
- Yun JY, Tamada Y, Kang YE, Amasino RM** (2012) *Arabidopsis* trithorax-related3/SET domain GROUP2 is required for the winter-annual habit of *Arabidopsis thaliana*. *Plant Cell Physiol* **53**: 834–846
- Zhang X, Bernatavichute YV, Cokus S, Pellegrini M, Jacobsen SE** (2009) Genome-wide analysis of mono-, di- and trimethylation of histone H3 lysine 4 in *Arabidopsis thaliana*. *Genome Biol* **10**: R62